

Performance Engineering for a Medical Imaging Application on the Intel Xeon Phi Accelerator

Johannes Hofmann
Chair of Computer Architecture
University Erlangen–Nuremberg
Email: johannes.hofmann@fau.de

Jan Treibig, Georg Hager, Gerhard Wellein
Erlangen Regional Computing Center
University Erlangen–Nuremberg
Email: jan.treibig@rrze.fau.de

Abstract—We examine the Xeon Phi, which is based on Intel’s Many Integrated Cores architecture, for its suitability to run the FDK algorithm—the most commonly used algorithm to perform the 3D image reconstruction in cone-beam computed tomography. We study the challenges of efficiently parallelizing the application and means to enable sensible data sharing between threads despite the lack of a shared last level cache. Apart from parallelization, SIMD vectorization is critical for good performance on the Xeon Phi; we perform various micro-benchmarks to investigate the platform’s new set of vector instructions and put a special emphasis on the newly introduced vector gather capability. We refine a previous performance model for the application and adapt it for the Xeon Phi to validate the performance of our optimized hand-written assembly implementation, as well as the performance of several different auto-vectorization approaches.

I. INTRODUCTION

The computational effort of 3D image reconstruction in Computed Tomography (CT) has required special purpose hardware for a long time. Systems such as custom-built FPGA-systems [1] and GPUs [2], [3] are still widely-used today, in particular in interventional settings, where radiologists require a hard time constraint for reconstruction. However, recently it has been shown that today even commodity CPUs are capable of performing the reconstruction within the imposed time-constraint [4]. In comparison to traditional CPUs the Xeon Phi accelerator, which focuses on numerical applications, is expected to deliver higher performance using the same programming models such as C, C++, and Fortran. Intel first began developing the many-core design (then codenamed Larrabee) back in 2006—initially as an alternative to existing graphics processors. In 2010 the original concept was abandoned and the design was eventually re-targeted as an accelerator card for numerical applications. The Xeon Phi is the first product based on this design and has been available since early 2013 with 60 cores, a new 512bit wide SIMD instruction set, and 8 GiB of main memory. This paper studies the challenges of optimizing the Feldkamp-Davis-Kress (FDK) algorithm for the Intel Xeon Phi accelerator. The fastest available CPU implementation from Treibig *et al.* [4] served as starting point for the Xeon Phi implementation. To produce meaningful and comparable results all measurements are performed using the RabbitCT benchmarking framework [5].

The paper is structured as follows. Section 2 will give an overview of previous work about the performance optimization of this algorithm. A short introduction to computed tomography is given in Section 3. Section 4 introduces the RabbitCT benchmark and motivates its use for this

study. Next we provide a hardware description of the Xeon Phi accelerator together with the results of various micro-benchmarks in Section 5. In Section 6 we give an overview of the implementation and the optimizations employed for the accelerator card. Section 7 contains a detailed performance model for our application on the Xeon Phi. The results of our performance engineering efforts are presented in Section 8; for the sake of completeness we also present the results obtained with compiler-generated code. Finally we compare our results with the fastest published GPU implementation and give a conclusion in Section 9.

II. RELATED WORK

Due to its medical relevance, reconstruction in computed tomography is a well-examined problem. As vendors for CT devices are constantly on the lookout for ways to speed up the reconstruction time, many computer architectures have been evaluated over time. Initially products in this field used special purpose hardware based on FPGA and DSP designs [1]. The Cell Broadband Engine, which at the time of its release provided unrivaled memory bandwidth, was also subject to experimentation [6], [7]. It is noteworthy that CT reconstruction was among the first non-graphics applications that were run graphics processors [2].

However, the use of varying data sets and reconstruction parameters limited the comparability of all these implementations. In an attempt to remedy this problem, the RabbitCT framework [5] provides a standardized, freely available CT scan data set and a uniform benchmarking interface that evaluates both reconstruction performance and accuracy. Current entries in the RabbitCT ranking worth mentioning include *Thumper* by Zinsser and Keck [3], a Kepler-based implementation which currently dominates all other implementations, and *fastrabbit* by Treibig *et al.* [4], a highly optimized CPU-based implementation.

III. COMPUTED TOMOGRAPHY

In diagnostic and interventional computed tomography an X-ray source and a flat-panel detector positioned on opposing ends of a gantry move along a defined trajectory—mostly a circle or helix—around the patient; along the way X-ray images are taken at regular angular increments. In general 3D image reconstruction works by back projecting the information recorded in the individual X-ray images (also called projection images) into a 3D volume, which is made up of individual

voxels (volume elements). In medical applications, the volume almost always has an extent of 512^3 voxels. To obtain the intensity value for a particular voxel of the volume from one of the recorded projection images we forward project a ray originating from the X-ray source through the isocenter of the voxel to the detector; the intensity value at the resulting detector coordinates is then read from the recorded projection image and added to the voxel. This process is performed for each voxel of the volume and all recorded projection images, yielding the reconstructed 3D volume as the result.

IV. RABBITCT BENCHMARKING FRAMEWORK

Comparing different optimized FDK implementations found in the literature with respect to their performance can be difficult, because of variations in data acquisition and preprocessing, as well as different geometry conversions and the use of proprietary data sets. The RabbitCT framework [5] was designed as an open platform that tries to remedy the previously mentioned problems. It features a benchmarking interface, a prototype back projection implementation, and a filtered, high resolution CT dataset of a rabbit; also included is a reference volume that is used to derive various image quality measures. The preprocessed dataset consists of 496 projection images that were acquired using a commercial C-arm CT system. Each projection is 1248×960 pixels wide and stores the X-ray intensity values as single-precision floating-point numbers. In addition, each projection comes with a projection matrix $A \in \mathbb{R}^{3 \times 4}$, which is used to perform the forward projection. The framework takes care of all required steps to set up the benchmark, so the programmer can focus entirely on the actual back projection implementation, which is provided as a module (shared library) to the framework.

A slightly compressed version of the unoptimized reference implementation that comes with RabbitCT is shown in Listing 1. This code is called once for every projection image. The three outer `for` loops (lines 2–4) are used to iterate over all voxels in the volume; note that we refer to the innermost `x`-loop, which updates one “line” of voxels in the volume, as line update kernel. The loop variables `x`, `y`, and `z` are used to logically address all voxels in memory. To perform the forward projection these logical coordinates used for addressing must first be converted to the World Coordinate System (WCS), whose origin coincides with the isocenter of the voxel volume; this conversion happens in lines 6–8. The variables `O` and `MM` that are required to perform this conversion are precalculated by the RabbitCT framework and made available to the back projection implementation in a `struct` pointer that is passed to the back projection function as a parameter. After this the forward projection is performed using the projection matrix A in lines 10–12. In order to transform the affine mapping that implements the forward projection into a linear mapping homogeneous coordinates are used. Thus the detector coordinates are obtained in lines 14 and 15 by dehomogenization.

In the next step a bilinear interpolation is performed. In order to do so, detector coordinates are converted from floating-point to integer type (lines 17 and 18), because integral values are required for addressing the projection image buffer `I`. The interpolation weights `scalex` and `scaley` are calculated in lines 20 and 21. The four values needed for the

```

// iterate over all voxels in the volume
for (z = 0; z < L; ++z) {
    for (y = 0; y < L; ++y) {
        for (x = 0; x < L; ++x) {
            // convert to WCS
            float wx = O+x*MM;
            float wy = O+y*MM;
            float wz = O+z*MM;
            // forward projection
            float u = wx*A[0]+wy*A[3]+wz*A[6]+A[9];
            float v = wx*A[1]+wy*A[4]+wz*A[7]+A[10];
            float w = wx*A[2]+wy*A[5]+wz*A[8]+A[11];
            // dehomogenize
            float ix = u/w;
            float iy = v/w;
            // convert to integer
            int iix = (int)ix;
            int iiy = (int)iy;
            // calculate interpolation weights
            float scalex = ix-iix;
            float scaley = iy-iiy;
            // load values for bilinear interpolation
            float valbl = 0.0f; float valbr = 0.0f;
            float valtr = 0.0f; float valt1 = 0.0f;
            if (iix >= 0 && iiy < width &&
                iix >= 0 && iix < height)
                valbl = I[iiy * width + iix];
            if (iiy >= 0 && iiy < width &&
                iix+1 >= 0 && iix+1 < height)
                valbr = I[iiy * width + iix + 1];
            if (iiy+1 >= 0 && iiy+1 < width &&
                iix >= 0 && iix < height)
                valt1 = I[(iiy + 1) * width + iix];
            if (iiy+1 >= 0 && iiy+1 < width &&
                iix+1 >= 0 && iix+1 < height)
                valtr = I[(iiy + 1) * width + iix + 1];
            // perform bilinear interpolation
            float valb = (1-scalex)*valbl+scalex*valbr;
            float valt = (1-scalex)*valt1+scalex*valtr;
            float val = (1-scaley)*valb+scaley*valt;
            // add distance-weighted results to voxel
            VOL[z*L*L+y*L+x] += val/(w*w);
        } // x-loop
    } // y-loop
} // z-loop

```

Listing 1. UNOPTIMIZED REFERENCE BACK PROJECTION IMPLEMENTATION PROCESSING A SINGLE PROJECTION IMAGE.

bilinear interpolation are fetched from the buffer containing the intensity values in lines 25–36. The `if` statements make sure, that the detector coordinates lie inside of the projection image; for the case where the ray doesn’t hit the detector, i.e. the coordinates lie outside the projection image an intensity value of zero is assumed (lines 23 and 24). Note that the two-dimensional projection image is linearized, which is why we need the projection image width in the variable `width`—also made available by the framework via the `struct` pointer passed to the function—to correctly address data inside the buffer. The actual bilinear interpolation is performed in lines 38–40.

Before the result is written back into the volume (line 42), it is weighed according to the inverse-square law. The variable `w`, which holds the homogeneous coordinate w , contains an approximation of the distance from X-ray source to the voxel

under consideration and can be used to perform the weighting.

V. INTEL XEON PHI

An overview of the Xeon Phi 5110P is provided in Figure 1. The main components making up the accelerator are the 60 cores connected to the high bandwidth ring interconnect through their Core–Ring Interconnects (CRI); interlaced with the ring is a total of eight memory controllers that connect the processing cores to main memory as well as PCIe logic that communicates with the host system.

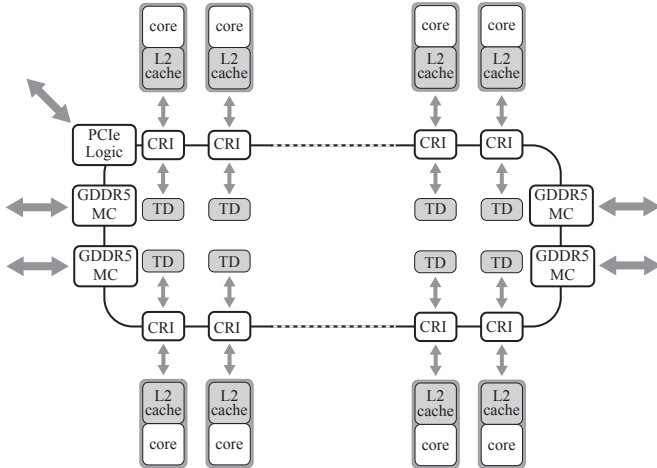


Fig. 1. SCHEMATIC OVERVIEW OF THE XEON PHI 5110P ACCELERATOR.

The cores are based on a modified version of the P54C design used in the original Pentium released in 1995. Each core is clocked at 1.05 GHz and is a fully functional, in-order core, which supports fetch and decode instructions from four hardware thread execution contexts—twice the amount used in recent x86 CPUs. The superscalar cores feature a scalar pipeline (V-pipe) and a vector pipeline (U-pipe). Connected to the U-pipe is the Vector Processing Unit (VPU), which implements the new Initial Many Core Instructions (IMCI) vector extensions.

A. Core Pipeline

The cores used in the Xeon Phi are in-order, lacking all of the necessary logic to manage out-of-order execution, making the individual cores less complex than their traditional CPU counterparts. A core can execute two instructions per clock cycle: one on the V-pipe, which executes scalar instructions, prefetches, loads, and stores; and one on the U-pipe, which can only execute vector instructions.¹ The decode unit is shared by all hardware contexts of a core and is a pipelined two-cycle unit to increase throughput. This means it takes the unit two cycles to decode one instruction bundle (i.e. one micro-op for the U- and one for the V-pipe); however, due to its pipelined design the unit can deliver decoded bundles to *different* hardware threads each cycle. As a consequence, at least two hardware threads must be run on each core to achieve peak performance; using only one thread per core will in the best case result in 50% of peak performance. We found,

¹Actual simultaneous execution is governed by a set of non-trivial pairing rules [8].

however, that it is good practise to always use all four hardware threads of a core because most vector instructions have a latency of four clock cycles and data hazards can be avoided without instruction reordering when using four threads.

B. Cache Organization, Core Interconnect, and Memory

Most of Intel’s cache concepts were adopted into the Xeon Phi: the Cache Line (CL) size is 64 bytes and cache coherency is implemented across all caches using the MESI protocol with the help of the distributed Tag Directory (TD). Each core includes a 32 KiB L1 instruction cache, a 32 KiB L1 data cache, and a unified 512 KiB L2 cache.

The L1 cache is 8-way associative and has a 1 cycle latency for scalar loads and a 3 cycle latency for vector loads. Its bandwidth has been increased to 64 bytes per cycle, which corresponds exactly to the vector register width of 512 bits. In contrast to recent Intel x86 CPUs which contain two hardware prefetching units for the L1 data cache (streaming prefetcher and stride prefetcher), there exist no hardware prefetchers for the L1 cache on the Xeon Phi. As a consequence, the compiler/programmer has to make heavy use of software prefetching instructions—which are available in various flavors (cf. Table I)—to make sure data is present in the caches whenever needed.

TABLE I. AVAILABLE SCALAR PREFETCH INSTRUCTIONS FOR THE INTEL XEON PHI.

Instruction	Cache Level	Non-temporal	Exclusive
<code>vprefetchnta</code>	L1	Yes	No
<code>vprefetch0</code>	L1	No	No
<code>vprefetch1</code>	L2	No	No
<code>vprefetch2</code>	L2	Yes	No
<code>vprefetchnta</code>	L1	Yes	Yes
<code>vprefetche0</code>	L1	No	Yes
<code>vprefetche1</code>	L2	No	Yes
<code>vprefetche2</code>	L2	Yes	Yes

Apart from standard prefetches into the L1 and L2 caches (`vprefetch0`, `vprefetch1`), there exist also variants that prefetch data into what Intel refers to the L1/L2 non-temporal cache (`vprefetchnta`, `vprefetch2`). Data prefetched into these non-temporal caches is fetched into the n th way (associativity-wise) of the cache, where n is the context id of the prefetching hardware thread and made MRU—i.e. the most recently used data will be replaced first. Prefetches can also indicate the requested CL be brought into the cache for writing, i.e. in the exclusive state of the MESI protocol (`vprefetche*`).

The L2 cache is 8-way associative and has a latency of 11 clock cycles. The size of the L2 cache is twice the size of recent Intel x86 designs, namely 512 KiB. The L2 cache contains a rudimentary streaming prefetcher that can only detect strides up to 2 CLs apart.

The Xeon Phi contains a total of eight dual-channel GDDR5 memory controllers clocked at 5 GHz, yielding a theoretical peak memory bandwidth of 320 GiB/s. To get an estimate of the attainable bandwidth for our application, we ran a streaming “Update” kernel which resembles the memory access pattern of our application (cf. Figure 2). We found that peak memory performance can only be achieved by employing

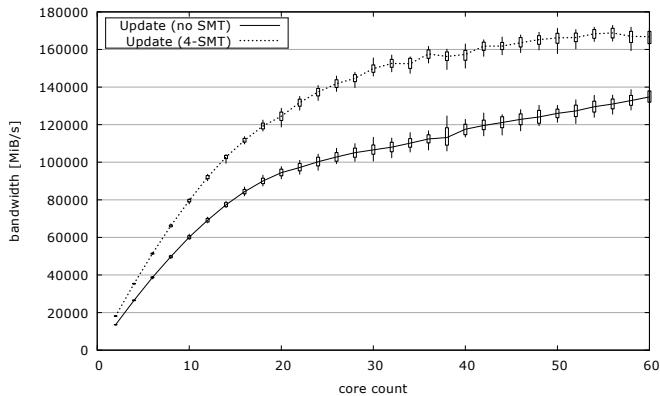


Fig. 2. MEMORY BANDWIDTH OF STREAMING UPDATE KERNEL.

SMT. The bandwidth of about 165 GiB/s corresponds to around 52% of the theoretical peak performance; this can be attributed to limited scalability of the memory system: the gradient of the graph is steeper for e.g. 10–20 cores than it is for e.g. 50–60 cores.

C. Initial Many Core Instructions

While AVX2—the latest set of vector instructions for Intel x86 CPUs—provides a total of 16 vector registers, each 256 bits wide, IMCI offers 32 registers, each 512 bits wide. IMCI supports fused-multiply add operations, yielding a maximum of 16 DP (32 SP) Flops per instruction. In addition to increasing the register count and width, IMCI also introduces eight vector mask registers, which can be used to mask out SIMD lanes in vector instructions; this means that a vector operation is performed only selectively on some of the elements in a vector register. Another novelty is the support for vector scatter and gather operations.

D. Vector Gather Operation

In the FDK algorithm, a lot of data has to be loaded from different offsets inside the projection image. The Intel Xeon Phi offers a vector gather operation that enables filling of vector registers with scattered data. A major advantage over sequential loads is the fact that vector registers can be used for addressing the data; this means no detour of writing the contents of vector registers to the stack to move them into scalar registers required for sequential loads is necessary.

```

..L100: vgatherdps zmm6{k3}, [rdi+zmm13*4]
        jkzd      k3, ..L101
        vgatherdps zmm6{k3}, [rdi+zmm13*4]
        jkznd    k3, ..L100
..L101:

```

Listing 2. GATHER PRIMITIVE IN ASSEMBLY. NB PARTICULAR CODE USING TWO BRANCHES SHOWN HERE GENERATED BY C INTRINSIC.

At first glance (cf. Listing 2), a `vgatherdps` instruction looks similar to a normal load instruction. In the example `zmm6` is the vector registers in which the gathered data will be stored. The `rdi` register contains a base address, `zmm13` is a vector register holding 16 32 bit integers which serve as offsets, and 4 is the scaling factor. The 16 bits of the

vector mask register act as a write mask for the operation: if the n th bit is set to 1 the gather instruction will fetch the data pointed at by the n th component of the `zmm13` register and write it into the n th component of the `zmm6` register; if the bit is set to 0 no data will be fetched and the n th component of `zmm6` is not modified. When a gather instruction is executed, only data from *one* CL is fetched. This means that when the data pointed at by the `zmm13` register is distributed over multiple CLs the gather instruction has to be executed multiple times. To determine whether all data has been fetched, the gather instruction will zero out the bits in the vector mask register whenever the corresponding data was fetched. In combination with the `jkznd` and `jkzd` instructions—which perform conditional jumps depending of the contents of the vector mask register—it is possible to form loop constructs to execute the gather instruction as long as necessary to fetch all data, i.e. until the vector mask register contains all zero bits.

TABLE II. LATENCIES IN CLOCK CYCLES OF THE VECTOR GATHER PRIMITIVE.

Distribution	L1 Cache		L2 Cache	
	Instruction	Loop	Instruction	Loop
16 per CL	9.0	9.0	13.6	13.6
8 per CL	4.2	8.4	9.4	18.8
4 per CL	3.7	14.8	9.1	36.4
2 per CL	2.9	23.2	8.6	68.8
1 per CL	2.3	36.8	8.1	129.6

A set of micro-benchmarks for `likwid-bench` from the `likwid` [9] framework were devised to measure the cycles required to fetch data using gather loop constructs; Table II shows the results, taking into account distribution of data across CLs. We find that the latency for a single gather instruction varies depending on how many elements it has to fetch from a CL. This might be taken as a hint that a single gather instruction itself is implemented as yet another loop, this time in hardware—the larger the number of elements that have to be fetched from a single CL, the higher the latency.

Table III summarizes the hardware specifications of the Xeon Phi and integrates them with two state of the art reference systems from the CPU and GPU domain.

VI. IMPLEMENTATION

Our implementation makes use of all the optimizations found in the original `fastrabbit` implementation [4]. As part of this work, we improved the original clipping mask optimization² by 10%. Another improvement we made was to pass function parameters inside vector registers to the kernel in accordance with the Application Binary Interface [10]: instead of replicating values from scalar registers onto the stack and then loading them into vector registers we directly pass the parameters inside vector registers.

While register spilling was a problem in the original implementation, the Xeon Phi with its 32 vector registers can handle all calculations without spilling. The number arithmetic instructions can be greatly reduced by the use of the

²For some projection angles several voxels are not projected onto the flat-panel detector. For these voxels a zero intensity is assumed. Such voxels can be “clipped” off by providing proper start and stop values for each x-loop.

TABLE III. HARDWARE SPECIFICATIONS OF THE INTEL XEON PHI AND TWO STATE OF THE ART CPU AND GPU REFERENCE SYSTEMS.

Microarchitecture Model	IvyBridge-EP Xeon E5-2660 v2	Knights Corner Xeon Phi 5110P	Kepler Tesla K20 (GK110)
Clock	2.2 GHz	1.05 GHz	0.706 GHz
Sockets/Cores/Threads per Node	2/20/40	1/60/240	1/13/-
SIMD support	8 SP/4 DP	16 SP/8 DP	192 SP/64 DP
Peak TFlop/s	0.70 SP/0.35 DP	2.02 SP/1.01 DP	3.52 SP/1.17 DP
Node L1/L2/L3 cache	20×32 KiB/20×256 KiB/20×2.5 MiB	60×32 KiB/60×512 KiB/-	13×48 KiB + 13×48 KiB (read-only)/1.5 MiB/-
Node Main Memory Configuration	2×4 ch. DDR3-1866	16 ch. GDDR5 5 GHz	10 ch. GDDR5 5.2 GHz
Node Peak Memory Bandwidth	119.4 GiB/s	320 GiB/s	208 GiB/s

fused multiply-add instructions (cf. lines 6–8, 10–12, 38–40, and 42). All divides are replaced with multiplications of the reciprocal; the reciprocal instruction on the Xeon Phi provides higher accuracy than current CPU implementations and is fully pipelined.

All projection data required for the bilinear interpolation are fetched using gather loop constructs. Several unsuccessful attempts to improve the L1 hit rate of the gather instructions were made. We found that the gather hint instruction, `vgatherpf0hintdps`, is implemented as a dummy operation—it has no effect whatsoever apart from instruction overhead. Another prefetching instruction, `vgatherpf0dps`, appeared to be implemented exactly the same as the actual gather instruction, `vgatherdps`: instead of returning control back to the hardware context after the instruction is executed, we found that control was relinquished only *after* the data has been fetched into the L1 cache, rendering the instruction useless. Finally, scalar prefetching using the `vprefetch0` instruction was evaluated. The problem with this approach is getting the $4 \cdot 16$ offsets stored inside a vector register into scalar registers. This requires storing the contents of the vector register onto the stack and sequentially loading them into general purpose registers. Obviously, 4 vector stores, as well as 64 scalar loads and prefetches, amounting to a total of 132 scalar instructions, is too much instruction overhead. As a consequence we evaluated variants in which only every second (68 instructions), fourth (36 instructions), or eighth (20 instructions) component of the vector registers was prefetched. Nevertheless, the overhead still outweighed any benefits caused by increasing the L1 hit rate.

Because the application is instruction throughput limited, dealing with the `if` statements (cf. lines 25–36 in Listing 1) using the zero-padding optimization³ results in better performance than the usage of predicated instructions, which incur additional instructions to set the vector mask registers.

Despite the strictly sequential streaming access pattern inside the volume the lack of a L1 hardware prefetcher mandates the use of software prefetching. We also find that using software prefetching for the L2 cache results in a much better performance than relying on the L2 hardware prefetcher. For the volume data, we used prefetching with the exclusive hint, because the voxel data will be updated. In addition, we deliberately fetch the volume data into the non-temporal portion of the L1 and L2 caches, because we know the volume

³Zero-padding refers to an optimization involving allocating a buffer that is large enough to “catch” all projection rays that miss the detector; the original projection image is copied into the buffer and the remainder of the buffer if filled with zero intensity values. The `if` statements to check whether the projected rays lie inside the projection image are thus no longer necessary.

is too large⁴ to fit inside the caches; this way, the volume data will not preempt cached projection data. For prefetched data be available when needed it is important to fetch the data in time. For our application, we achieved best performance when prefetching volume data four loop iterations before accessing them from main memory into the L2 cache and one loop iteration ahead from the L2 into to L1 cache.

Efficient OpenMP parallelization requires more effort on the Xeon Phi than on traditional CPUs. While even on today’s high-end multi-socket CPU systems the number of hardware threads is usually below 100, the Xeon Phi features 240 hardware threads. On CPUs it was sufficient to parallelize the outermost `z`-loop (cf. line 2 in Listing 1) and use a static scheduling with chunk size of 1 to work around the imbalances created by the clipping mask. This way each thread is updating one plane of the volume a time. On the Xeon Phi this distribution of work would result in 208 of the 240 threads updating two planes and 32 of the threads updating three planes. In other words 208 threads would be idle 33% of the time. The solution is to make the amount of work more fine-granular, while at the same time ensuring the amount of work will not become so small that the overall runtime is dominated by overhead. To make the work more fine-granular the OpenMP collapse directive was used to fuse the `z` and `y` loops. The optimum chunk size was empirically determined to be 262—corresponding to about half a plane in the volume.

Another important consideration on the Xeon Phi is thread placement. The default “scatter” thread placement, in which thread 0 is run on core 0, thread 1 on core 1, etc. and SMT threads of cores are only used when all physical cores have been exhausted proves unfit for our application. With this scattered placement threads that run on the same physical core have no spatial locality in the volume; as a result they do not have a spatial locality in the projection image, which leads to preemption of projection data in the core’s caches (which is shared among the hardware contexts of the core). Using “gather” thread placement in which thread 0 runs on hardware context 0 of core 0, thread 1 on context 1 of core 0, etc. we ensure spatial locality inside the volume and the projection data thus reducing cache preemptions.

VII. PERFORMANCE MODEL

Popular performance models like the Roofline model [11] reduce investigations to determining whether kernels are compute- or memory-bound, not taking runtime contributions of the cache subsystem into account.

⁴The volume memory footprint is $512^3 \text{ Voxels} \cdot 4 \text{ bytes/Voxel} = 512 \text{ MiB}$.

The performance model we use is based on a slightly modified version of the model used in the original *fastrabbit* publication [4], [12]. At the basis of the model is the execution time required to update the 16 voxels in a single CL, assuming all data is available in the L1 cache. In addition, the contribution of the cache and memory subsystem is modeled, which accounts for time spent transferring all data required for the update into the L1 cache and back. In the original model, designed for out-of-order CPUs, an estimation whether the cache subsystem overhead can be hidden by overlapping it with the execution time is given and the authors conclude that there exist sufficient suitable instructions⁵ to hide any overhead caused by in-cache transfers. However, in their analysis, Treibig *et al.* only consider the in-cache contribution of the CLs relating to the voxel volume; all CLs pertaining to the projection images, required for the bilinear interpolation, are assumed to reside in the L1 cache. On the Intel Xeon Phi we find this simplification no longer holds true. There is a non-negligible cost for transferring the projection data from the L2 to the L1 cache that can not be overlapped with the execution time.

A. Core Execution Time

Unfortunately there exist no tools such as, e.g., the Intel Architecture Code Analyzer (IACA) [13], which is used to measure kernel execution times on Intel’s CPU microarchitectures, for the Intel Xeon Phi. Therefore, we have to perform a manual estimation of the clock cycles spent in a single iteration of the line update kernel—which corresponds to the update of one CL. To complicate things, simply counting the instructions in the kernel is not an option, because the number of gather instructions varies depending on the distribution of the data to be fetched across CLs. As a consequence, we begin with an estimation of the execution time for a gather-less kernel (i.e. a version of the line update kernel in which all gather loop constructs have been commented out).

Manually counting the instructions, we arrive at 34 clock cycles for a gather-less kernel iteration. This analytical estimation was verified by measurement. For one voxel line containing 512 voxels a runtime of 2402 clock cycles was measured using a single thread. This corresponds to 75 clock cycles per kernel iteration (when one iteration updates 16 voxels). Taking into account that the single thread can only issue instruction every other clock cycle, the core execution time for one loop iteration is approximately 37.5 clock cycles—which is a close fit to the value of 34 clock cycles determined previously. For our model, we use the measured value of 37.5 clock cycles because it contains non-negligible overhead that was not accounted for in the analytical value.⁶

To estimate the contribution of the gather loop constructs we first determine how often a gather instruction is executed on average for a CL update. To get this value, we divide the total

⁵Because the L1 cache is single-ported—i.e. it can only communicate with either the core or the L2 cache at any given clock cycle—transfers between the L1 and L2 caches can only overlap with “suitable” instructions that do not access the L1 cache such as, e.g., arithmetic instructions with register operands.

⁶The overhead includes the time it takes to call the line update kernel (backing up and later restoring callee-save registers, the stack base pointer, etc. onto the stack) as well as instructions in the kernel that are not part of the loop body, such as resetting the loop counter.

number of gather instructions issued during the reconstruction (obtained by measurement) by total number of loop iterations. We find that, on average, the gather instruction is executed 16 times in a kernel iteration. Distributing that number over the four gather loop constructs (one for each of the four values required for the bilinear interpolation) we arrive at 4 gather instructions per gather loop—indicating that the data is, on average, distributed across four CLs. From this we can infer the runtime contribution based on our previous findings (cf. Table II). The latency of each gather instruction in the situation where the data is distributed across four CLs is 3.7 clock cycles. With a total of 16 gather instructions per iteration, the contribution is 59.2 clock cycles. Together with the remaining part of one kernel loop iteration (37.5 clock cycles), the total execution time is approximately 97 clock cycles.

B. Cache and Memory Subsystem Contribution

To estimate the impact of the runtime spent transferring the data required for the CL update we first have to identify which transfers can not be overlapped with execution time. As previously established the voxel volume is too large for the caches. Thus each CL of the volume has to be brought in from main memory for the update; eventually, the updated CL will also have to be evicted. This means that a total of 2 CLs, corresponding to 128 byte, have to be transferred. Using software prefetching any latency and transferring cost from the memory and cache subsystems regarding volume data can be avoided.

As previously discussed, prefetching the projection data is not possible without serious performance penalties. Using *likwid-perfctr* from the *likwid* framework [9] we investigated the Xeon Phi’s performance counters and found that 88.5% of the projection data can be serviced from the local L1 cache and the remaining 11.5% can be serviced from the local L2 cache. Since each gather is transferring a full CL, this amounts to approximately $16 \text{ CLs} \cdot 64 \text{ byte/CL} \cdot 11.5\% \approx 118 \text{ byte}$. We estimate the *effective* L2 bandwidth in conjunction with the gather instruction to be the following: the latency of a single gather instruction (when dealing with data that is distributed across four CLs) was previously measured to be 3.7 clock cycles with data in L1 cache, respectively 9.1 clock cycles with data in the L2 cache (cf. Table II). Assuming the difference of 5.4 clock cycles to be the exclusive L2 cache contribution, we arrive at an effective bandwidth of $64 \text{ byte}/5.4 \text{ cycle} = 11.85 \text{ byte/cycle}$. The average memory subsystem contribution is thus $118 \text{ byte}/11.85 \text{ byte/cycle} \approx 10 \text{ cycles}$.

Figure 3 provides an overview of the performance model. The upper part shows core and L1 cache, together with all data transfers from the cache. The lower part shows the memory hierarchy through which data has to be transferred to perform the CL update. The arrows to the left represent the CLs pertaining the voxel volume data; prefetching these CLs in time guarantees overlap of transfers with core execution. The arrow to the right between the L1 and L2 caches represents the transfers of projection data which can not be prefetched; the latency of these transfers is the determining factor for the memory subsystem contribution. This leads to a total of 107 clock cycles to perform a single CL update.

Based on the runtime of a single kernel iteration we can determine whether the memory bandwidth becomes a limiting

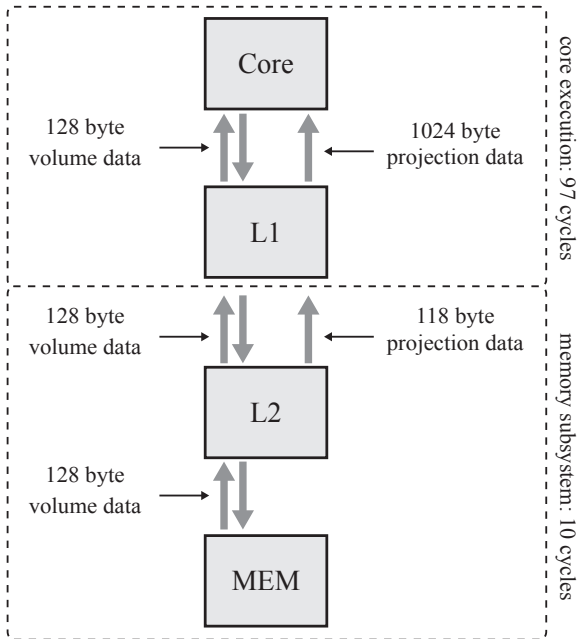


Fig. 3. OVERVIEW OF EXECUTION TIME AND MEMORY SUBSYSTEM CONTRIBUTION.

factor for our application. For each loop iteration, 128 byte (2 CLs) have to be transferred over the memory interfaces. Each of the 60 cores is clocked at 1.05 GHz; at 107 cycles per iteration, the required bandwidth is:

$$\frac{1.05 \text{ GHz/core}}{107 \text{ cycles}} \cdot 60 \text{ cores} \cdot 128 \text{ byte} = 70.0 \text{ GiB/s.}$$

The required value is well below the measured sustainable bandwidth of around 165 GiB/s (cf. Fig. 2), indicating that bandwidth is not a problem for our application.

Given the model, the total runtime contribution of the line update kernel is

$$\frac{4.39 \cdot 10^{10} \text{ voxels}}{16 \text{ voxels/iteration}} \cdot \frac{107 \text{ cycles/iteration}}{60 \text{ cores} \cdot 1.048 \text{ GHz/core}} = 4.67 \text{ s.}^7$$

Unfortunately, there is a non-negligible amount of time spent outside of the line update kernel. The value obtained by measuring the runtime of the reconstruction with the call to the kernel commented out was 0.42 s. Thus, the total reconstruction time is 5.09 s. Foreclosing the runtime of the assembly implementation from the next section which is 5.16 seconds (cf. Table IV) we estimate the model error at 1.4%.

VIII. RESULTS AND DISCUSSION

In addition to our hand-written assembly implementation we also evaluated several auto-vectorization approaches for the FDK kernel: native vectorization using the Intel C Compiler, the only recently introduced vectorization directive from the latest OpenMP 4 standard [14] implemented in the Intel

⁷The total number of voxels to process is given by considering each voxel of the clipped volume once for each of the 496 projection images.

TABLE IV. RUNTIMES AND PERFORMANCE OF ALL IMPLEMENTATIONS FOR A 512^3 VOLUME.

Version	time [s]	Performance [GUp/s]
OpenMP 4 (<code>#pragma simd</code>)	7.77	5.6
ISPC (Version 1.5.0)	7.00	6.3
Intel C Compiler (Version 13.1.3)	6.99	6.3
Assembly	5.16	8.5

Compiler, and the Intel SPMD Program Compiler (ISPC) [15]. Table IV shows the runtime in seconds and the corresponding performance in Giga Voxel Updates per Second (GUp/s)—the commonly used performance metric for FDK—of all implementations. All implementations were benchmarked using static OpenMP scheduling with a chunk size of 262 voxel lines; independent of the implementation, this value resulted in the best performance.

We find that the performance of auto-vectorization variants can not match the speed of our manually written assembly kernel. Even the best of the three variants—the native vectorization of the Intel C Compiler—can only provide around 74% of the performance of hand-written code. We find that the performance provided by the latest version of the free, open-source ISPC almost matches that of the commercial Intel C Compiler; the original ISPC version that was used during the early stages of this work had a 10% lower performance. The result obtained with the OpenMP 4 directive was the worst; the main reason is that the standard guarantees the results obtained with this vectorization are identical to that of scalar code—thus prohibiting several optimizations, such as reordering of arithmetic instructions to increase performance.

Our performance model revealed that even in the ideal case in which all projection data resides in the L1 cache, the runtime impact of gathering the projection data (59.2 cycles) dominates the overall runtime of a kernel iteration (97 cycles). We thus identify the gather operation as the limiting factor for this application. While all other parts of the FDK kernel benefit from the increase of the vector register width at the same time the increased width counteracts the performance, because the cost of filling the vector registers with scattered data increases linearly with register width.

IX. CONCLUSION

We have presented a detailed examination of the Intel Xeon Phi accelerator by performing various benchmarks. We performed various optimizations for the FDK algorithm and devised a manually vectorized assembly implementation for the Xeon Phi and compared it to auto-vectorized code. In order to integrate our findings with today’s state of the art reconstruction implementations a comparison of our implementations with an improved⁸ version of the *fastrabbit* implementation, as well as the fastest currently available GPU implementation called *Thumper* [3] is shown in Table V.

We find that the Kepler-based GeForce GTX 680 by Nvidia can perform the reconstruction 7–8 times faster, depending on the volume’s discretization. This discrepancy can not be explained by simply examining the platforms’ specifications

⁸Back-porting various optimizations of the Xeon Phi implementations yielded a 25% increase in performance for the *fastrabbit* CPU implementation.

TABLE V. COMPARISON OF DIFFERENT PLATFORMS IN GUP/s.

Platform	Version	512 ³	1024 ³
2S-Xeon E5-2660	<i>improved fastrabbit</i>	6.2	6.7
Xeon Phi 5110P	OpenMP 4 (#pragma simd)	5.6	5.7
	ISPC (Version 1.5.0)	6.3	6.4
	Intel C Compiler (Version 13.1.3)	6.3	6.4
	Assembly	8.5	13.1
GeForce GTX 680	<i>Thumper</i>	67.7	88.2

such as peak Flop/s and memory bandwidth. The main causes contributing to the GPU's superior performance for this particular application are discussed in the following.

Most computations involved in the reconstruction kernel, such as the projection of voxels onto the detector panel or the bilinear interpolation, are typical for graphics applications (which GPUs are designed for). While, due to the fused multiply-add operation, the forward projection is performed efficiently on both the GPU and the Xeon Phi platform, the bilinear interpolation is not. GPUs possess additional hardware called texture units, each of which can perform a bilinear interpolation using a single instruction for data inside the texture cache. To emphasize the implications, consider that out of the total of 97 clock cycles for one loop iteration of the FDK kernel, 6 cycles are used for the computation of the detector coordinates and 3 cycles to weight the interpolated intensity value and update the voxel volume; the remaining 88 clock cycles, more than 90% of the kernel, is spent on the bilinear interpolation⁹—which is handled by a single instruction on a GPU.

Given a sufficient amount of work, Nvidia's CUDA programming model does a better job at hiding latencies. As seen before, even in the ideal case where all data can be serviced from the L1 cache, on average, each of the gather instructions has a latency of 3.7 clock cycles. Although the Intel Xeon Phi can hide the latencies of most instructions when using all four hardware contexts of a core, 4-way SMT is not sufficient to hide latencies caused by loading non-continuous data. In contrast to SMT, Nvidia's multiprocessors feature hardware that allows them to instantly switch between warps.¹⁰ This way, every time a warp has to wait for an instruction to complete or data to arrive from the caches or main memory, the hardware simply schedules another warp in the meantime. Given a sufficient number of warps to choose from, this approach can hide much higher latencies than the 4-way SMT in-order approach.

Although we have shown that the Intel Xeon Phi accelerator can not provide the same performance as GPUs for the task of 3D reconstruction in the interventional setting, there nevertheless might be applications that can benefit from our work. One promising application seems to be the reconstruction of large CT volumes. Today, the largest industrial CT scanner, which at the time of this writing is the XXL-CT device only recently installed by the Fraunhofer Institute in Fürth [16], is capable of recording projection images with a resolution

⁹This includes preparing the interpolation weights, converting floating-point detector coordinates to integral values, gathering the projection data, and performing the actual interpolation.

¹⁰On Nvidia GPUs, the number of CUDA threads concurrently executing on a core is called warp.

of 10000×10000 pixels, corresponding to more than 380 MiB per projection image. In this setting, it is possible for main memory capacity and bandwidth to play more important roles, potentially giving CPUs, with their high memory capacities, and the Intel Xeon Phi, with its high memory bandwidth, an advantage over GPUs. Another interesting topic of research, of course, will be to evaluate the next iteration of the Intel Xeon Phi architecture, codenamed Knights Landing, for this application once it becomes available.

REFERENCES

- [1] B. Heigl and M. Kowarschik, "High-speed reconstruction for C-arm computed tomography," in *In Proceedings Fully 3D Meeting and HPIR Workshop*, July 2007, pp. 25–28.
- [2] G. Pratz and L. Xing, "Gpu computing in medical physics: A review," *Medical Physics*, vol. 38, no. 5, pp. 2685–2697, 2011. [Online]. Available: <http://link.aip.org/link/?MPH/38/2685/1>
- [3] T. Zinsser and B. Keck, "Systematic Performance Optimization of Cone-Beam Back-Projection on the Kepler Architecture," in *Proceedings of the 12th Fully Three-Dimensional Image Reconstruction in Radiology and Nuclear Medicine*, F. committee, Ed., 2013, p. 225228.
- [4] J. Treibig, G. Hager, H. G. Hofmann, J. Hornegger, and G. Wellein, "Pushing the limits for medical image reconstruction on recent standard multicore processors," *International Journal of High Performance Computing Applications*, 2012, (Accepted). [Online]. Available: <http://arxiv.org/abs/1104.5243>
- [5] C. Rohkohl, B. Keck, H. Hofmann, and J. Hornegger, "RabbitCT - an open platform for benchmarking 3D cone-beam reconstruction algorithms," *Medical Physics*, vol. 36, no. 9, pp. 3940–3944, 2009.
- [6] M. Kachelriess, M. Knaup, and O. Bockenbach, "Hyperfast parallel-beam and cone-beam backprojection using the cell general purpose hardware," *Med Phys*, vol. 34, no. 4, pp. 1474–86, 2007. [Online]. Available: [Http://www.biomedsearch.com/nih/Hyperfast-parallel-beam-cone-backprojection/17500478.html](http://www.biomedsearch.com/nih/Hyperfast-parallel-beam-cone-backprojection/17500478.html)
- [7] H. Scherl, M. Kowarschik, H. G. Hofmann, B. Keck, and J. Hornegger, "Evaluation of state-of-the-art hardware architectures for fast cone-beam ct reconstruction," *Parallel Comput.*, vol. 38, no. 3, pp. 111–124, Mar. 2012.
- [8] "Intel Xeon Phi Coprocessor Vector Microarchitecture." [Online]. Available: <http://software.intel.com/sites/default/files/article/393199/intel-xeon-phi-coprocessor-vector-microarchitecture.pdf>
- [9] J. Treibig, G. Hager, and G. Wellein, "LIKWID: A lightweight performance-oriented tool suite for x86 multicore environments," in *PST2010, the First International Workshop on Parallel Software Tools and Tool Infrastructures*. Los Alamitos, CA, USA: IEEE Computer Society, 2010, pp. 207–216. [Online]. Available: <http://dx.doi.org/10.1109/ICPPW.2010.38>
- [10] Intel Corporation, *System V Application Binary Interface — K10M Architecture Processor Supplement*, April 2012.
- [11] S. W. Williams, A. Waterman, and D. A. Patterson, "Roofline: An insightful visual performance model for floating-point programs and multicore architectures," EECS Department, University of California, Berkeley, Tech. Rep. UCB/EECS-2008-134, Oct 2008.
- [12] J. Treibig and G. Hager, "Introducing a performance model for bandwidth-limited loop kernels," in *Parallel Processing and Applied Mathematics*, ser. Lecture Notes in Computer Science, R. Wyrzykowski, J. Dongarra, K. Karczewski, and J. Wasniewski, Eds. Springer Berlin / Heidelberg, 2010, vol. 6067, pp. 615–624.
- [13] "Intel architecture code analyzer." [Online]. Available: <http://software.intel.com/en-us/articles/intel-architecture-code-analyzer/>
- [14] OpenMP Architecture Review Board, *OpenMP Application Program Interface — Version 4.0*, July 2013.
- [15] M. Pharr and W. R. Mark, "ispc: A SPMD Compiler for High-Performance CPU Programming," in *In Proceedings Innovative Parallel Computing (InPar)*, San Jose, CA, May 2012.
- [16] "Fraunhofer Institute, XXL-CT." [Online]. Available: <http://www.iis.fraunhofer.de/de/bf/xrt/system/xxl-ct.html>